A Study about Turning Three-Phase Electrical Motors in Active Magnetic Bearings

Christian Tshizubu[a], José Andrés Santisteban [a,b]

[a] Graduate Program on Mechanical Engineering (PGMEC), Universidade Federal Fluminense (UFF), Rua Passo da Pátria 156, Niterói, Brazil, ctshizubu@yahoo.fr
[b] Graduate Program on Electrical and Telecommunications Engineering (PPGEET), UFF, Rua Passo da Pátria 156, Niterói, Brazil, jasantisteban@ieee.org

***Abstract*—Nowadays, the operation principle of active magnetic bearings (AMB's) is well known and their industrialization can be considered mature. Nevertheless, spreading this technology around all the world is yet a tough work as its actual production cost is even high. Taking an operative rotational machine, by instance, in the process of a substitution of mechanical bearings by magnetic ones, as the mechanical details are customized, the stator construction cost can be quite expensive. In this sense, in order to save time and reduce costs, an alternative approach has been studied. This consists on turning conventional AC electrical motors in AMB's. Different from a previous reported work, where a two-phase induction motor was modified and experimentally tested, in this work, a three-phase induction motor is studied through Finite Elements Analysis. Its distributed windings structure is unchanged while the rotor is substituted by another one without a squirrel cage. To simulate the AMB behavior, two conditions were evaluated: first, two phase windings were supplied, while the third one was kept open, and second, all the three phase windings were supplied. Finally, the equivalent net forces were evaluated as a function of differential control currents, holding the rotor centralized, and also as a function of the radial displacements, holding all the windings currents constant. Simulation results show that supplying the three windings is desirable from the point of view of the radial displacement control.**

I. INTRODUCTION

Nowadays, the technology of active magnetic bearings (AMB) is found in several applications [1]. Many of the reported experiences are related to complete manufactured equipments where AMB's are part of them. Nevertheless, in some cases, the possibility of only substitute mechanical bearings by magnetic units, in a conventional rotative machine, is a challenge. In that case, the stator, rotor and airgap dimensions of the AMB have to be appropriately designed. Anyway, as choosing a disposable market unit is not always a trivial task, a customized construction is almost frequently the necessary and high cost work.

In this sense, the authors have been studying an alternative approach to diminish the cost of the mechanical construction of AMB's. This is based in the use of a common electrical machine to turn its behavior similar to an AMB.

The first experience was experimentally tested in a four-poles squirrel cage induction motor that dispose of two-phase stator windings, distributed along 24 slots, as depicted in Fig. 1.

In this case, only the phase A was utilized and the squirrel cage rotor was substituted by another one, with the same dimensions, but disposing of a laminated structure [2], [3], as depicted in Fig. 2.

This approach is different to the reported since the 80's [4], [5], where a bearingless motor, with split windings, was the main research objective. Nevertheless, the operation principle to generate radial forces from the interconnected magnetic fluxes with four poles, is hold.

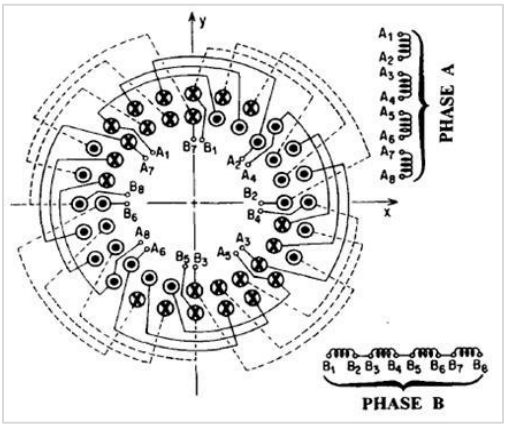

Figure 1. Stator winding to achieve radial magnetic force [2], [3].

Figure 2. Shaft with laminated silicon steel rotor [3].

In this paper, a four poles three-phase induction motor, like the shown in Fig. 3, with a higher number of slots (36) is studied. In Fig. 4, a double layer winding distribution, with each winding occupying 6 slots, i.e, 3 in the outer layer and 3 in the inner layer, is shown and in Fig. 5, all their 12 individual components in a star connection are shown. All the outer terminals are connected to the terminal "O"

Based on this structure, the open source software FEMM 4.2 [6] was utilized as a Finite Elements tool. For two different possibilities, the radial magnetic forces were evaluated and compared.

Figure 3. Stator of a three-phase induction motor with 36 slots [7].

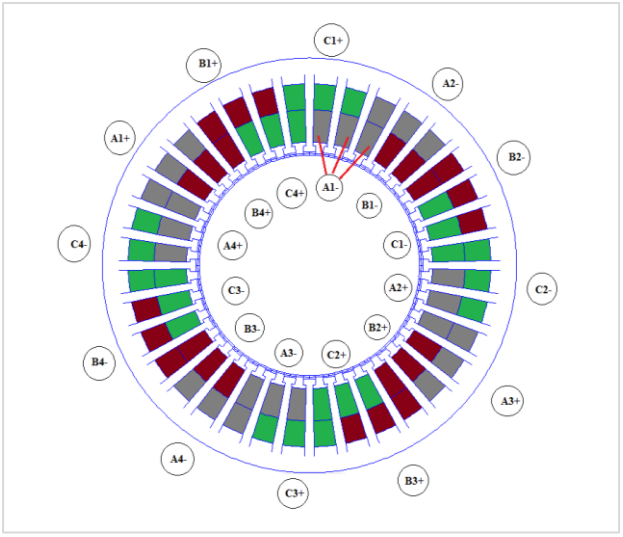

Figure 4. Winding distribution of the 36 slots three-phase stator.

At first, all the 3 phases (A, B and C) were supplied with DC currents. It was named the SIGMA case. At second, only 2 phases (B and C) were supplied, while the remaining one was held open. This case was named the BETA case.

In Table I, the geometrical dimensions of the simulated structure is shown.

TABLE I. Geometrical dimensions

Parameter	Value
Outer stator diameter	128 mm
Inner stator diameter	72 mm
Rotor diameter	70 mm
Nominal airgap	1 mm
Depth	85 mm

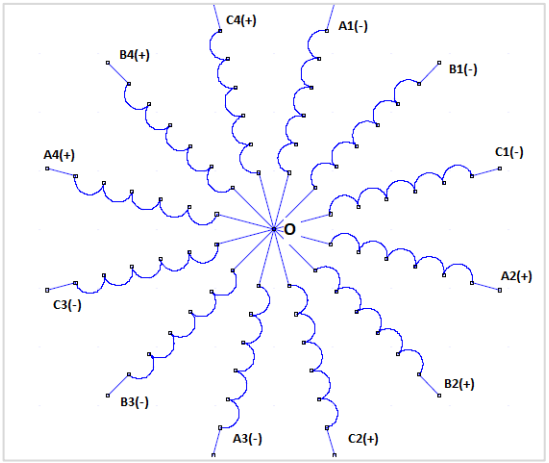

Figure 5. Schematic winding distribution to achieve radial magnetic forces using a four poles structure by phase..

II. MODELING

In order to understand the contribution of this work, it is necessary to briefly remind the basic concepts related to the radial magnetic forces generated by the electromagnetic device under study.

As known, the net radial magnetic force can be obtained through the derivation of the virtual work, according to the Maxwell principles [8], as shown in (1):

$$F = \frac{dW_e}{dh} = \frac{1}{2}[i]^T \frac{\partial[\lambda]}{\partial h} = \frac{1}{2}[i]^T \frac{\partial[L]}{\partial h}[i] \qquad (1)$$

Where *dWe* is the variation of the stored magnetic energy, λ is the flux linkages vector, whose components are defined in (2), [*i*] is the currents vector with dimension 12x1, [*L*] is the symmetrical matrix of inductances of dimension 12x12; *h* is any displacement along a reference axis.

$$\lambda_j = \sum_j L_{jk} * i_k \quad (2)$$

Where *j,k* depends on the particular winding: A1, A2, A3, A4, B1, B2,B3, B4, C1, C2, C3 or C4.

As it will be discussed in the next section, the net magnetic forces are aligned with new "*x*" and "*y*" axes, which are displaced by a certain angle in relation to initial suposed fixed Cartesian axes.

On the other hand, respect to the dynamic model of the electromechanical device, the one proposed in [9], (3) will be adopted for control purpose.

$$\ddot{Z}_s + G_r \dot{Z}_s - K_{zs} Z_s = K_{us} u \quad (3)$$

Where, Z_s is the states vector, $Z_s = [x\ y]^T$; $G_r = I^{-1}G$; $K_{zs} = k_x b^2 I^{-1}$; $K_{us} = k_i bc I^{-1}$; *I* is the inertial matrix, *G* is the gyroscopic matrix, *u* is the currents vector, *b* is the vertical height of the point where the magnetic force is applied to the rotor, *c* is the vertical height of the point where the displacement sensors capture the rotor displacements and finally, *kx* and *ki* are

respectively the displacement and current coefficients of the linearized model of the electromagnetic forces vector *F*, (4).

$$F = k_x Z_s + k_i u \quad (4)$$

The values of theses last coefficients are found in this paper applying the conditions of operation, discussed in the section IV.

III. Finite Elements Analysis

To illustrate the magnetic flux density during the evaluation of the analyzed cases in this paper, Fig. 6 and Fig. 7 depict the magnetic flux density for both SIGMA and BETA cases, for a condition of centralized rotor and a control current di of 0.2 A. In both cases the same number of turns, 96 per slot, was considered. However, they differ in the bias current, 0.295 A in the SIGMA case and 0.415 A in the BETA case. In this simulation, the M-19 silicon steel was used, being the linear limit of magnetic flux around of 1.5 T. In this way, both cases were forced to obtain the same current coefficient *ki*, as confirmed in Fig. 11. From this condition, an equivalent average MMF of 82 ampere-turns was obtained.

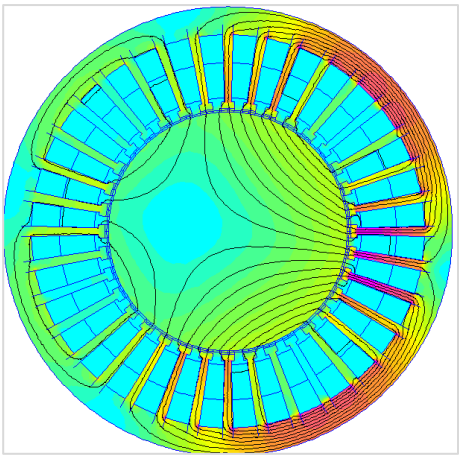

Figure 6. Magnetic flux density – SIGMA structure with di = 0.2 A.

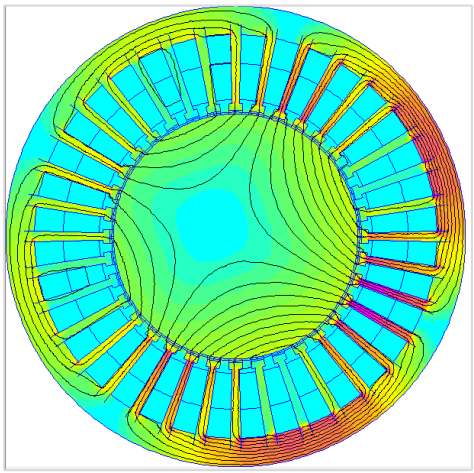

Figure 7. Magnetic flux density – BETA structure with di = 0.2 A.

On the other hand, Fig. 8 and Fig. 9 depict the magnetic flux density for both SIGMA and BETA cases, for a condition of equal currents for all the windings while the rotor is displaced 0.2 mm from its centralized condition.

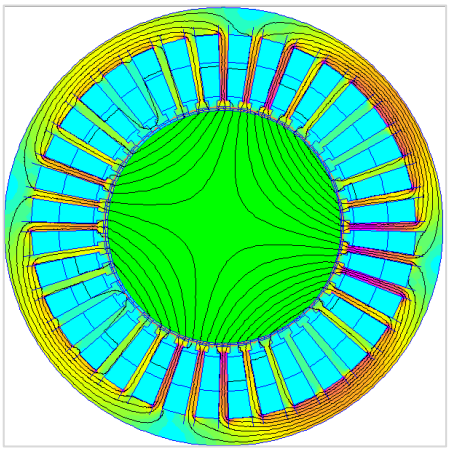

Figure 8. Magnetic flux density – SIGMA structure with dx = 0.2 mm.

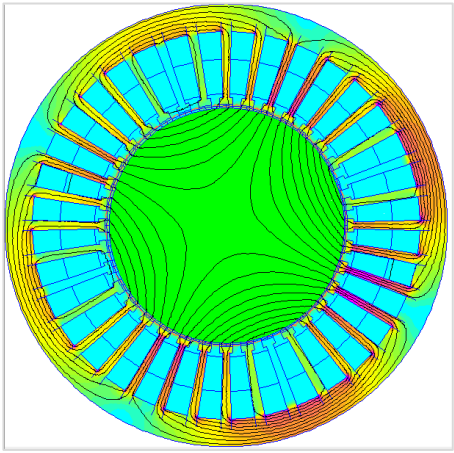

Figure 9. Magnetic flux density – BETA structure with dx = 0.2 mm.

IV. Simulation Results

As explained before, in order to evaluate the magnitude of the magnetic forces, and then, to obtain the displacement and current coefficients of the linearized model of the electromagnetic forces, *kx* and *ki*, two conditions were considered. At first, the rotor was kept centralized while the control currents were added and subtracted, respectively, to the opposed windings that contribute with the net forces generated. The final orientation of the magnetic forces, that defines the net equivalent x-axis, is depicted in Fig. 10. At second, the control current for all the windings was maintained null while the rotor was displaced along their net equivalent x-axis.

Fig. 11 depicts the results of the first condition. It can be observed that the net magnetic forces in both cases are similar so they have the same sensibility (*ki*) to variations of the control current *di*.

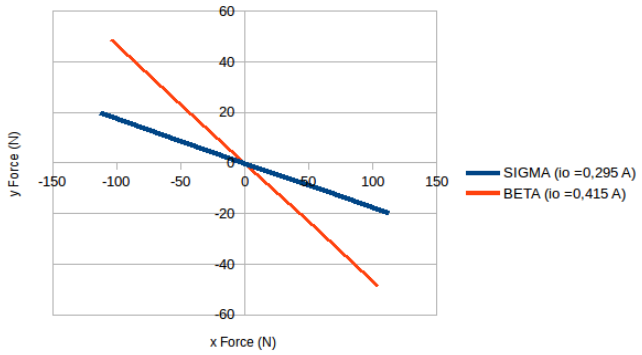

Figure 10. Net equivalent x-axis.

In Fig. 12, the results of the second condition are depicted. The magnetic forces for the BETA case are higher than for the SIGMA case, so the former has more sensibility (*kx*) to the rotor displacement than the later.

From Figs. 11 and 12, the ratio *ki*/*kx* for the SIGMA case was 3.66 while for the BETA case it was 2.97, which in terms of the postion control strategy, the SIGMA structure presents lower interference of the decentralized postion than the BETA case.

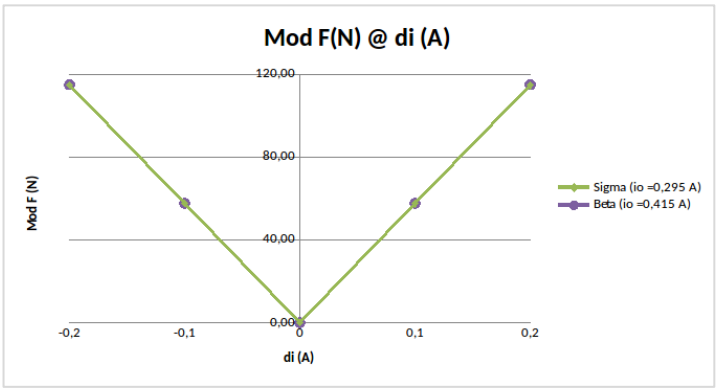

Figure 11. Magnetic Forces versus Control Current.

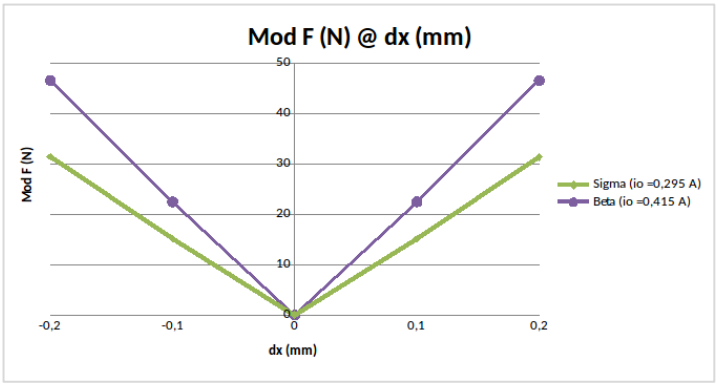

Figure 12. Magnetic Forces versus Rotor Displacement.

V. Conclusions

A different approach of magnetic bearings using conventional stator windings of a four poles three-phase induction motor has been presented. Only one structural change must be done in the rotor, i.e. it is substituted by another one without the squirrel cage.

Through Finite Element analysis, they were tested two possible strategies to generate radial magnetic forces. It was concluded that supplying all the three phase windings, instead of only two phase windings, has as advantage a lower influence of some rotor misalignment in the performance of a displacement controller.

Additionally, from the economical point of view of the mechanical construction, the authors have verified that the manufacturing of a set of stator and rotor of conventional active magnetic bearing, with similar dimensions, is six times higher than the cost to modify the rotor of the induction motor.

References

[1] www.magneticbearings.org, accessed in February 05th , 2018.

[2] C. Tshizubu, J. A. Santisteban, "A Simple PID Controller for a Magnetic Bearing with Four Poles and Interconnected Magnetic Flux", 2017 6th International Symposium on Advanced Control of Industrial Processes (AdCONIP), pp 430-435, 2017.

[3] C. Tshizubu, J. A. Santisteban, "Turning Induction Motors in Four Poles Active Magnetic Bearings with Coupled Fluxes", 2017 Brazilian Power Electronics Conference (COBEP), pp. 1-6, 2017.

[4] A. O. Salazar, R. M. Stephan, "A Bearingless Method for Induction Machines", IEEE Transactions on Magnetics, Vol. 29, No. 6, pp. 2965-2967, 1993.

[5] E. F. Rodriguez, J. A. Santisteban, "An Improved Control System for a Split Winding Bearingless Induction Motor", IEEE Transactions on Industrial Electronics, Vol. 58, No. 8, pp. 3401-3408, 2011.

[6] http://www.femm.info/wiki/HomePage, accesed in June 27th, 2018.

[7] http://winding.wixsite.com/design/buy-now?lightbox=c1ovn accessed in June 27th, 2018

[8] G. Schweitzer, H. Bleuer, A. Traxler, Magnetic Bearings: Theory, Design, and Application to Rotating Machinery, Springer, 1st Edition, 2009.

[9] R. M. Stephan, F. C. Pinto, A. C. Gomes, J. A. Santisteban, A. O. Salazar, Mancais magnéticos - Mecatrônica sem atrito, Editora Ciência Moderna, 2013.